# A Combined Waveform-Beamforming Design for Millimeter-Wave Joint Communication-Radar

Preeti Kumari\*, Nitin Jonathan Myers\*, Sergiy A. Vorobyov<sup>†</sup>, and Robert W. Heath, Jr.\*

\*Wireless Networking and Communication Group, ECE Department, The University of Texas at Austin, TX, USA

†Department of Signal Processing and Acoustics, Aalto University, Espoo, Finland

{preeti\_kumari, nitinjmyers, rheath}@utexas.edu, sergiy.vorobyov@aalto.fi

Abstract—Millimeter-wave (mmWave) joint communicationradar (JCR) simultaneously realizes a high data rate communication and a high-resolution radar sensing for applications such as autonomous driving. Prior JCR systems that are based on the state-of-the-art mmWave communications hardware, however, suffer from a limited angular field-of-view (FoV) and low detection rate for radars due to the employed directional beam. To address this limitation, we propose an adaptive and fast combined waveform-beamforming design for mmWave JCR with a phased-array architecture. We present a JCR beamformer design algorithm that permits a trade-off between communication data rate and radar successful recovery rate in the angular domain. We show that distinct radar measurements can be obtained with circulant shifts of the designed JCR beamformer for compressed radar sensing. Numerical results demonstrate that our JCR design enables the angle-of-arrival/departure estimation of shortrange radar targets with a high successful recovery rate and a wide FoV at the expense of a slight loss in the communication rate.

# I. INTRODUCTION

Joint communication-radar (JCR) uses a common transmit (TX) signal for both communication and radar operations to enable hardware and spectrum reuse. A solution to realize JCR for next-generation applications, such as autonomous driving, is to exploit the large bandwidth at the millimeter-wave (mmWave) band [1]. In [2], [3], a practical mmWave WiFi-based JCR was proposed during the data transmission mode to achieve Gbps data rate simultaneously with a high range and velocity estimation accuracy for long-range radar applications. Unfortunately, the angular field of view (FoV) for short-range radar (SRR) applications was limited due to the employed directional beam.

Prior approaches to increase the radar FoV for mmWave JCR can be categorized into three types: (a) JCR during the communication beam training mode, (b) JCR with an adaptive beamforming design during the data transmission mode, and (c) multiple-input-multiple-output JCR with low resolution analog-to-digital converters. In the first approach [4], the IEEE 802.11ad control physical (PHY) layer frames along with beam scanning algorithm during the beam training mode was proposed for radar sensing with a wide FoV. In the second approach [5], the IEEE 802.11ad single-carrier (SC) PHY frames along with the adaptive random switching (RS) of TX antennas during the data transmission mode was proposed. In the RS-JCR, a coherent beam is formed towards the communication receiver, while simultaneously perturbing the

grating lobes of the resulting beam pattern for angle-of-arrival (AoA) estimation in SRR applications. In the last approach [6], a mmWave multiple-input-multiple-output JCR with 1-bit analog-to-digital converters per RF chain was proposed to achieve a high range and AoA estimation accuracy. The RS-JCR has a higher radar update rate and communication data rate than the first approach, and is based on a commercially available mmWave hardware unlike the third approach. The RS-JCR, however, employs TX antenna subsets instead of using all antennas, which decreases the net TX power for JCR operation under a per-antenna power constraint.

In this paper, we develop an adaptive combined waveformbeamforming design that exploits all the TX and receive (RX) antennas for mmWave JCR during the data transmission mode. Our mmWave JCR design enables a highly accurate AoA and angle-of-departure (AoD) estimation of SRR targets in a wide FoV without reducing communication rate much. For reduced hardware complexity, we assume a phased-array architecture at both the TX and RX. In particular, we present a TX beamfomer design algorithm to generate a narrow coherent beam for communication and constant gain sidelobes in other directions for radar sensing. The TX beamfomer design accounts for the trade-off between the sidelobe gain for radar and the mainlobe gain for communication. The radar receiver acquires distinct radar channel measurements using circulant shifts of the designed beamformer. To quantify the JCR trade-off for an adaptive combined waveform-beamforming design, we use the data rate metric for communication and a novel successful recovery rate metric for radar. Numerical results demonstrate that our JCR design performs significantly better than the RS-JCR extended for both AoA and AoD estimation, especially for a large number of antennas.

**Notation**: The operators  $(\cdot)^*$  stands for conjugate transpose,  $(\cdot)^T$  for transpose, and  $(\bar{\cdot})$  for conjugate of a matrix or a vector.  $\mathcal{N}(\mu, \sigma^2)$  is used for a complex circularly symmetric Gaussian random variable with mean  $\mu$  and variance  $\sigma^2$ .  $\mathbf{A}\star\mathbf{B}$  is defined as the 2D circular cross-correlation between matrices  $\mathbf{A}$  and  $\mathbf{B}$  [7], whereas  $\langle \mathbf{A}, \mathbf{B} \rangle = \sum_{k,\ell} \mathbf{A}(k,\ell)\bar{\mathbf{B}}(k,\ell)$  is defined as the inner product of  $\mathbf{A}$  and  $\mathbf{B}$ .  $\mathbf{A}\odot\mathbf{B}$  is defined as the elementwise multiplication of  $\mathbf{A}$  and  $\mathbf{B}$ .

# II. SYSTEM MODEL

We consider the use case where a source vehicle sends a mmWave JCR waveform to communicate with a recipient

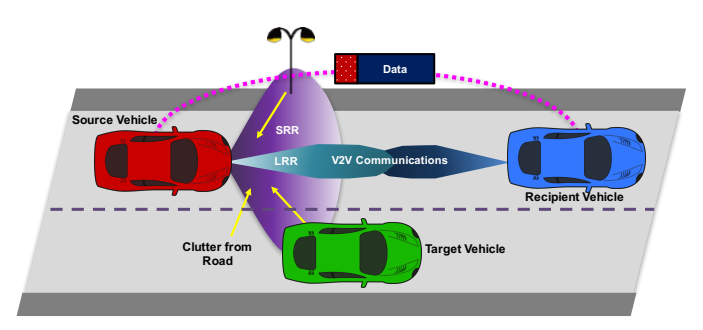


Figure 1: An illustration of an mmWave JCR system that simultaneously perform SRR sensing with a wide FoV and V2V communication with a narrow FoV.

vehicle at a distance  $d_c$ , while simultaneously using the received echoes for automotive radar sensing, as shown in Fig. 1. We consider closely separated TX antenna array and receive (RX) antenna array mounted on both source and recipient vehicles. For simplicity, we assume that the antenna arrays are uniform linear arrays with N-elements each. We assume a phased array architecture with q-bit phase shifters at the TX and the RX, where the phase shift alphabet is defined as  $\mathbb{Q}_q = \{e^{\mathrm{j}2k\pi/2^q}/\sqrt{N}: k \in \{1,2,3,\cdots N\}\}.$ 

We consider a coherent processing interval (CPI) of T seconds. During a CPI, we consider a SC PHY TX waveform structure with  $\mu$  fraction of training sequence symbols and  $1-\mu$  fraction of communication data symbols, similar to IEEE 802.11ad. The training sequence is assumed to consist of codes that possess good correlation properties for radar and channel estimation, such as Golay complementary sequences implemented in 60 GHz WiFi. The JCR channel model in our paper is similar to that of [5].

During a CPI, our JCR design uses an adaptive collection of TX and RX beams to achieve a high-resolution radar sensing in a wide FoV with a minimal reduction in the communication data rate. We propose to use  $\delta$  fraction of TX power along the communication receiver direction,  $\phi_0$ , and  $1-\delta$  fraction of TX power along the other directions for SRR sensing. Within a CPI, the transmitter sends M different combinations of TX precoder and RX beamformer vectors to acquire distinct SRR channel measurements. We denote the symbol period as  $T_{\rm s}$ , define a block of  $T/MT_{\rm s}$  symbols as a pulse, and denote the  $p^{\text{th}}$  JCR symbol in the  $m^{\text{th}}$  pulse as s[m, p]. The source vehicle transmits the symbols with the power constraint  $\mathbb{E}\left[|s[m,p]|^2\right] = \mathcal{E}_{s}$  and uses a unit norm TX beamforming vector  $\mathbf{f}(m, \delta)$  as well as a unit norm RX beamforming vector  $\mathbf{w}[m]$ . The receiver at the recipient vehicle employs a unit norm beamforming vector  $\mathbf{w}_{c}$ .

Communication received signal model: To explore the performance trade-off between communication and radar, we consider an illustrative example of a line-of-sight dominant narrowband mmWave communication channel between the source and recipient vehicles [5]. Nonetheless, the approach developed in this paper can be extended for different scattering scenarios by including non-line-of-sight communication channels; the extension is omitted because of space limitation.

The communication channel between the source and recipient vehicle is characterized by its channel gain,  $h_{\rm c}$ , which includes path loss, AoA/AoD pair  $(\phi_0,\theta_0)$ , path delay  $d_{\rm c}/c$  with c being the speed of light. For a linear array with elements half-wavelength spaced, we define the array steering vector as  $\mathbf{a}(\theta) = [1,e^{\mathrm{j}\pi\sin\theta},e^{\mathrm{j}2\pi\sin\theta},\cdots,e^{\mathrm{j}(N-1)\pi\sin\theta}]^T$ . Assuming perfect synchronization and additive noise  $e_{\rm c}[m,p] \sim \mathcal{N}(0,\sigma_{\rm c}^2)$ , the received communication signal with the TX steering vector  $\mathbf{a}(\theta_0)$ , the RX steering vector  $\mathbf{a}(\phi_0)$ , and the channel  $\mathbf{H}_{\rm c} = \sqrt{h_{\rm c}}\mathbf{a}(\phi_0)\mathbf{a}^*(\theta_0)$  is

$$y_{c}[m, p] = \mathbf{w}_{c}^{*} \mathbf{H}_{c} \mathbf{f}(m, \delta) s[m, p] + e_{c}[m, p]. \tag{1}$$

Assuming that the TX and RX beams are perfectly aligned and directional beamforming with a spatial matched filter is used at the RX to provide the maximum TX-RX array gain for the considered line-of-sight channel model, (1) simplifies as

$$y_{c}[m, p] = \sqrt{h_{c}\delta}Ns[m, p] + e_{c}[m, p].$$
 (2)

We define communication signal-to-noise ratio (SNR) corresponding to the ideal beampattern for communication with  $\delta=1$  as  $\zeta_{\rm c}=\mathcal{E}_{\rm s}h_{\rm c}N^2/\sigma_{\rm c}^2$ . The net received signal SNR increases linearly with the fraction of TX power for communication and is given by  $\delta\zeta_{\rm c}$ .

Radar received signal model: We represent the doubly selective (time- and frequency-selective) mmWave radar channel using virtual representation obtained by uniform sampling in range and Doppler dimensions [3]. Since the focus of this paper is target detection/estimation in the angular domain and not in the range/Doppler domain, we describe radar signal model for a particular dominant range-Doppler bin with distance d and velocity v after applying corresponding delay and Doppler shift compensation as in [5], [8].

The particular range-Doppler bin is assumed to consist of a few,  $K \ll N^2$ , virtual scattering centers that consist of  $K_{\rm t}$  targets and  $K-K_{\rm t}$  multi-path spread-Doppler clutter components. The  $k^{\rm th}$  virtual scattering center is described by its AoA/AoD pair  $(\phi_k,\theta_k)$  and complex channel gain  $\beta_k$ , which is a product of radar cross-section and path-loss. We define the radar channel as  $\mathbf{H} = \sum_{k=0}^{K-1} \sqrt{\beta_k} \mathbf{b}^c(\phi_k) \mathbf{a}^*(\theta_k)$ . Then, the radar signal obtained after cross correlating the TX training sequences with the received  $m^{\rm th}$  pulse echoes is

$$y[m] = \mathbf{w}^*[m]\mathbf{Hf}(m,\delta) + e[m], \tag{3}$$

where the additive noise is denoted by  $e[m] \sim \mathcal{N}(0, \sigma^2/\mathcal{E}_s \gamma)$ . The complex factor  $\gamma$  is the integration gain due to the employed cross-correlation, which depends on the training sequences used within a pulse of T/M duration. In numerical simulations, we consider the pulse to be a portion of a SC PHY frame, where the pilots comprising of Golay complementary sequences are used for correlation-based channel estimation. A pulse could also have been chosen to consist of several preambles in a CPI, but it would have degraded the communication rate due to a large increase in the total training sequence duration within this interval.

# III. BEAMFORMER DESIGN FOR JCR

In this section, we explain our approach to construct a collection of beamformers that are well suited to the JCR application. Our method first constructs one sequence for each of the TX and RX. These sequences are designed according to the JCR specification. Then, our method constructs the collection of beamformers by circularly shifting the sequences constructed at the TX and the RX. As circulant shifts of a vector preserve the magnitude of its discrete Fourier transform (DFT), the proposed method ensures that the beams constructed according to our procedure achieve the desired JCR specifications. The collection of circularly shifted beamformers help to acquire distinct radar channel measurements.

Now, we explain the key idea underlying the proposed transmit beamformer design technique. For tractability, we design the beamformer by considering a DFT grid with N discrete angles. For ease of exposition, we assume the communication direction is  $0^o$ . The transmit beamformer design problem in JCR is to design a sequence  $\mathbf{f}_0 \in \mathbb{Q}_q^N$  whose beampattern has an energy of  $\delta$  along  $0^\circ$ . The remaining energy in the beamformer must be distributed to enable radar channel reconstruction with fewer channel measurements. Prior work has shown that beamformers with close to uniform gain along the desired sensing directions enable fast channel reconstruction through compressed sensing [7]. To this end, the proposed construction distributes the energy of  $1-\delta$  "uniformly" across the remaining DFT grid locations.

We show here how the Gerchberg-Saxton (GS) algorithm [9] can be used to construct the desired TX beamformer. We define  $\delta_{\rm rad}=(1-\delta)/(N-1).$  The DFT magnitude vector associated with the desired beamformer is then  ${\bf b}_{\rm mag}=[\sqrt{\delta},\sqrt{\delta_{\rm rad}},\sqrt{\delta_{\rm rad}},\cdots,\sqrt{\delta_{\rm rad}}].$  The inverse DFT of  ${\bf b}_{\rm mag}$ , however, may not be an element in  $\mathbb{Q}_q^N$ . The GS algorithm is an alternating projection method that finds a sequence in  $\mathbb{Q}_q^N$  such that the magnitude of its DFT is close to  ${\bf b}_{\rm mag}.$  We use  ${\rm phase}_q(x)$  to denote the q- bit phase quantized version of x. The GS algorithm is summarized in Algorithm 1.

# **Algorithm 1** GS algorithm to find $f_0$

- 1: **Inputs:**  $\delta$ , N, q, and  $T_{GS}$ .
- 2: **Initialize:** Set  $t_{\text{iter}} = 1$  and  $\mathbf{f}_0$  to a Zadoff-Chu sequence.
- 3: while  $t_{\rm iter} < T_{\rm GS}$  do
- 4:  $\mathbf{b}_{\text{phase}} \leftarrow \text{phase} \left( \text{DFT}(\mathbf{f}_0) \right)$
- 5: Constraint on the discrete beam pattern:
  - $\mathbf{b} \leftarrow \mathbf{b}_{\text{mag}} \odot \exp(\mathsf{j}\mathbf{b}_{\text{phase}})$
- 6: Constraint on the antenna weights:
  - $\mathbf{f}_{\text{phase}} \leftarrow \text{phase}_q \left( \text{IDFT}(\mathbf{b}) \right)$
- 7:  $\mathbf{f}_0 \leftarrow \exp(\mathbf{j}\mathbf{f}_{\text{phase}})/\sqrt{N}$
- 8: end while
- 9: **return**  $\mathbf{f}_0$ .

The proposed GS-based beamformer design procedure can be generalized for any communication direction  $\theta \neq 0^{\circ}$ . The transmit beamformer in such a case is defined as  $\mathbf{f}_0 \odot \mathbf{a}(\theta)$ .

For the radar receiver, a good compressed sensing (CS)-based beamformer is one that has equal energy at all DFT-grid locations [7]. We propose to use a Zadoff-Chu sequence in  $\mathbb{Q}_q^N$  to be the RX combiner vector  $\mathbf{w}_0$  because the DFT of a Zadoff-Chu sequence has a constant amplitude.

# IV. COMPRESSED SENSING USING THE DESIGNED BEAMFORMERS

Now, we explain how radar channel measurements are acquired using the beamformers  $\mathbf{f}_0$  and  $\mathbf{w}_0$ . The radar channel  $\mathbf{H} \in \mathbb{C}^{N \times N}$  encodes the AoA and AoD information of the targets, and it is sparse at mmWave. The sparse channel  $\mathbf{H}$  can be reconstructed from fewer measurements according to the model in (3). The measurements in the proposed CS technique are acquired by applying random circulant shifts of  $\mathbf{f}_i = \mathbf{J}_i \mathbf{f}_0$  and  $\mathbf{w}_j = \mathbf{J}_j \mathbf{w}_0$  at the TX and the RX, where  $\mathbf{J}_i$  is the  $i^{\text{th}}$  circulant-delay matrix. Such a CS technique is known as convolutional CS [10], [11]. The base matrix in convolutional CS is defined as  $\mathbf{B}_{i,j} = \mathbf{w}_j^* \mathbf{f}_i$ . Therefore, the noiseless measurement corresponding to  $\mathbf{f}_i$  and  $\mathbf{w}_j$  is given as

$$z[i,j] = \mathbf{w}_i^* \mathbf{H} \mathbf{f}_i = \langle \mathbf{H}, \mathbf{w}_j \mathbf{f}_i^* \rangle = \langle \mathbf{H}, \mathbf{B}_{i,j} \rangle.$$
(4)

The received measurements when the TX and the RX apply all combinations of circulant shifts can be represented as  $\mathbf{Z} = \mathbf{H} \star \mathbf{B}_{0,0}$ . We assume that 2D-DFT of  $\mathbf{H}$ , defined as  $\mathbf{X}$ , is k-sparse. Using the properties of the 2D-DFT, the 2D-DFT of  $\mathbf{Z}$  can be expressed as  $\mathbf{S} = \mathbf{X} \odot \mathbf{D}$ , where  $\mathbf{D}$  is the 2D-DFT of  $\mathbf{B}_{0,0}$ . As  $\mathbf{X}$  is k-sparse, it can be shown that  $\mathbf{S}$  is at most k-sparse. Such a property can be exploited to recover  $\mathbf{S}$  from fewer projections than  $N^2$ .

In 2D-convolutional CS, the TX and RX apply  $M \ll N^2$  distinct pairs of circulant shifts of  $\mathbf{f}_0$  and  $\mathbf{w}_0$ . We define  $\Omega$  as a set containing the pair of circulant shifts used at the RX and the TX. For example, M=3 and  $\Omega=\{(0,0),(1,2),(2,1)\}$ . The operator  $\mathcal{P}_{\Omega}(\mathbf{A}) \to \mathbb{C}^M$  returns the entries of a matrix  $\mathbf{A}$  at the locations in  $\Omega$ . The noisy radar channel measurements with convolutional CS can be expressed as

$$\mathbf{y} = \mathcal{P}_{\Omega}(\mathbf{Z}) + \mathbf{e},\tag{5}$$

where the additive noise e[m] is defined in (3).

Next, we describe a CS algorithm and corresponding recovery guarantees to estimate  ${\bf H}$  from the channel measurements in (5). A reasonable approach for radar channel estimation is to minimize the  $\ell_1$  norm of  ${\bf S}$  subject to the constraint corresponding to (5). Such a method encourages channels that are faithful to the measurements in (5) and whose 2D-DFT is sparse [10]. Let  $\hat{{\bf H}}$  be the solution to the  $\ell_1$  minimization program and  $D_{\min}$  denote the minimum magnitude of  ${\bf D}$ , i.e., the 2D-DFT of  ${\bf B}_{0,0}$ . For the construction in Section III, it can be shown that  $D_{\min} = \sqrt{\delta_{\rm rad}}$ . We use [7, Theorem 1] to obtain a guarantee on the radar channel reconstruction performance.

**Theorem 1.** For a fixed constant  $\epsilon \in (0,1)$ , the solution  $\hat{\mathbf{H}}$  obtained with  $\ell_1$  norm minimization over  $\mathbf{S}$  satisfies

$$\|\mathbf{H} - \hat{\mathbf{H}}\|_F \le C_1 \frac{N\sigma}{\sqrt{\delta_{\text{rad}}}},$$
 (6)

with a probability of at least  $1 - \epsilon$  if  $M \ge Ck \max \{2\log^3(2k)\log(N), \log(\epsilon^{-1})\}$ . The constants C and  $C_1$  are independent of all the other parameters.

*Proof.* The result follows by using the assumption that X is k-sparse and the fact that  $D_{\min} = \sqrt{\delta_{\mathrm{rad}}}$  in [7, Theorem 1].  $\square$ 

The bound in (6) indicates that sparse radar channels can be recovered from sub-linear channel measurements that are acquired using the proposed beamformers. The result in Theorem 1 also indicates that the MSE of the channel estimate scales inversely with  $\delta_{\rm rad}$ , i.e., the fraction of energy used for sensing in JCR.

In numerical simulations, we show that the sparse matrix **S** can be efficiently recovered from a subsampled version of **Z** using a low-complexity OMP algorithm that exploits the partial 2D-DFT nature of our radar CS problem [10].

#### V. PERFORMANCE METRICS

We consider achievable data rate,  $R_c(\delta)$ , as the performance metric for the communication system in (2) with  $\delta$  as the fraction of TX power for communication. For  $\delta=1$ , we achieve maximum effective SNR at the communication receiver,  $\zeta_c$ , and maximum data rate using the ideal beampattern for communication. Assuming  $s_c[n,p]$  is distributed as  $\mathcal{N}_{\mathbb{C}}(0,1)$ , the maximum achievable data rate is given by

$$R_{\rm c}(\delta) = \frac{1}{T_{\rm s}} \log_2 \left( 1 + \delta \zeta_{\rm c} \right). \tag{7}$$

For radar performance evaluation of the proposed JCR system with a probability of successful recovery,  $P_{\rm r}(\delta,M)$ , in a CPI of T seconds, we define a novel normalized radar successful recovery rate metric as

$$R_{\rm r}(\delta, M) = \frac{P_{\rm r}(\delta, M)}{\eta_{\rm r} M T_{\rm int}},\tag{8}$$

where  $\eta_{\rm r}$  is the normalization factor. The metric  $R_{\rm r}(\delta,M)$  is analogous to the detection rate metric [12], which is used to study the trade-off between integration time and scanning rate. We choose  $\eta_{\rm r}$  such that the maximum value of  $R_{\rm r}(\delta,M)$  is 1 for better interpretation of the radar detection results.

The trade-off curve for our JCR combined waveform-beamforming design can be obtained using the data-rate constrained problem with a minimum required data rate  $\Upsilon_{\rm c}$ , which is given as

$$\label{eq:maximize} \begin{split} & \max_{\delta} & R_{\mathrm{r}}(\delta, M) \\ & \text{subject to} & R_{\mathrm{c}}(\delta) \geq \Upsilon_{\mathrm{c}} \\ & & \mathbf{W} \in \mathcal{W}(\delta) \\ & & \mathbf{F} \in \mathcal{F}(\delta) \\ & & M \geq Ck \mathrm{log}^3(2k) \log(N), \end{split}$$

where  ${\bf F}$  is the matrix of M TX precoder vectors and  ${\bf W}$  is the matrix of M RX precoder vectors at the source vehicle during a CPI. The TX codebook  ${\cal F}(\delta)$  and the receive codebook  ${\cal W}(\delta)$  are based on our JCR beamformer design described in Sections III and IV.

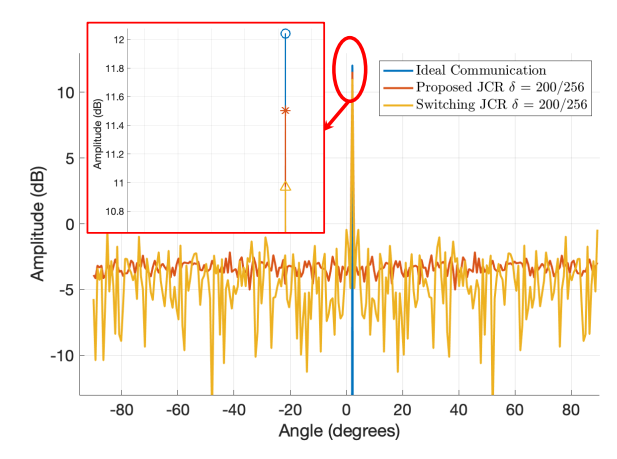


Figure 2: Comparison between the TX beampattern achieved by our JCR design with RS-JCR and the ideal communication. Our JCR achieves higher mainlobe gain than RS-JCR for data communication under a per-antenna power constraint.

# VI. NUMERICAL RESULTS

In this section, the numerical results of the proposed adaptive combined waveform-beamforming design for mmWave JCR are presented. The TX/RX antenna arrays are considered to be uniform linear arrays with 256 elements. We assume the grid size of 256 with 180° FoV, the recipient vehicle distance  $d_{\rm c}=100$  m, and the radar cross-section as 10 dBsm [13]. The interval for one independent TX-RX beam pair is considered as  $T_{\rm int}=0.2$  ms. We employed the OMP algorithm [7] for its simplicity to estimate the support of virtual radar channel in the angular domain, X.

Fig. 2 compares the TX beampattern for ideal communication, our proposed JCR with  $\delta = 200/256$ , and the RS-JCR proposed in [5] with the number of TX antennas switched on as 200. We see that communication TX power achieved by our proposed JCR using GS-algorithm improves by 1 dB as compared to the RS-JCR. The mainlobe for both the JCR beampatterns, however, has reduced gain compared to the ideal communication beampattern. Therefore, the best communication rate would be achieved by the ideal communication, followed by our JCR, and lastly the RS-JCR. The sidelobe gains achieved by the ideal communication beampattern, however, is the lowest and results in the worst radar performance. We observe random sidelobes with several grating lobes and nulls for the RS-JCR, whereas we observe constant sidelobe gain for our proposed JCR. Additionally, over an ensemble of beamformers constructed according to our JCR design, the net TX power along SRR directions is smaller for the RS-JCR than that for our proposed JCR.

Fig. 3 shows the variation of probability of successful recovery with the number of measurements and antennas for both the proposed JCR and the extended RS-JCR for AoA/AoD estimation. The extended RS-JCR is realized by incorporating phase randomization in the RX combiner vector in addition to the RS at the TX proposed in [5]. We see that our proposed JCR needs much lesser number of measurements than the RS-JCR to achieve a high probability of successful

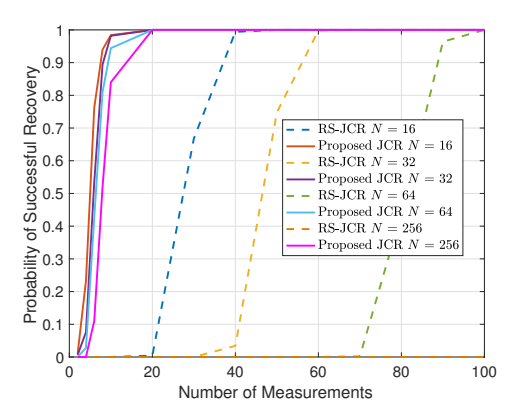


Figure 3: Comparison of RS-JCR with our proposed JCR for varying number of measurements and antennas at d = 12 m and  $\delta = 200/256$ . Our JCR performs better than the RS-JCR.

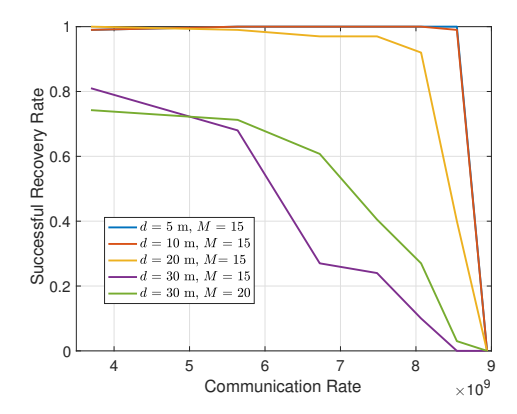


Figure 4: The trade-off curve achieved by our JCR with N = 256 with  $\eta_{\rm r} = 1/(15~T_{\rm int})$ . The radar successful recovery rate improves with decreasing  $\delta$ , while lowering  $R_{\rm c}(\delta)$ .

recovery. The difference between the radar successful recovery rate achieved by these approaches increases with the number of antennas. Our proposed JCR achieves the probability of successful recovery close to one within a CPI of less than 10 ms, which is desirable in automotive radars [13].

Fig. 4 shows the trade-off curve between communication rate,  $R_{\rm c}(\delta)$ , and radar successful recovery rate,  $R_{\rm r}(\delta,M)$ , with different values of  $0.1 \leq \delta \leq 1$  for N=256. The radar successful recovery rate improves with decreasing  $\delta$  due to increase in the radar SNR, while lowering communication data rate due to decrease in the communication SNR. From Fig. 4, we observe that the radar successful recovery rate for a given communication rate reduces with distance. For a distance of 30 m, although  $P_{\rm r}(\delta,M)=0.99$  for M=20 and  $P_{\rm r}(\delta,M)=0.82$  for M=15 at  $\delta=0.1$  with  $R_{\rm c}(\delta)=4$  Gbps,  $R_{\rm r}(\delta,M)$  is higher for M=15 than M=20. Additionally, we can see from Fig. 4 that large M is preferred at low  $\delta$ , whereas small M is preferred at high  $\delta$  for our JCR design.

# VII. CONCLUSION

In this paper, we proposed a TX-RX JCR beamformer design for the mmWave JCR system with a phased-array architecture to estimate radar AoA/AoD with a wide FoV at

the cost of a small reduction in communication data rate. Our AoA and AoD estimation technique for SRR targets exploits mmWave channel sparsity and has a low complexity due to the partial DFT CS. Our proposed TX precoder and RX combiner design for mmWave JCR performs better than the random switching-based one, especially for a large number of antennas. The results in this paper can be used to develop low-power, small size, spectrum-efficient, and high-performance mmWave devices that will enable next-generation automotive sensing and communication needs. Future work includes an extension of our work for simultaneous range, velocity, and direction estimation, as well as experimental demonstration.

# ACKNOWLEDGMENT

We thank Dr. Mohammed E. Eltayeb of California State University for discussions on 2D-angle estimation for RS-JCR. This material is based upon work supported in part by the National Science Foundation under Grant No. ECCS-1711702 and the U.S. Department of Transportation through the Data-Supported Transportation Operations and Planning (D-STOP) Tier 1 University Transportation Center.

# REFERENCES

- [1] K. V. Mishra, M. R. Bhavani Shankar, V. Koivunen, B. Ottersten, and S. A. Vorobyov, "Toward millimeter-wave joint radar communications: A signal processing perspective," *IEEE Signal Process. Mag.*, vol. 36, no. 5, pp. 100–114, Sep. 2019.
- [2] P. Kumari, N. Gonzalez-Prelcic, and R. W. Heath Jr, "Investigating the IEEE 802.11ad Standard for Millimeter Wave Automotive Radar," in Proc. IEEE Veh. Technol. Conf., September 2015, pp. 3587–3591.
- [3] P. Kumari, J. Choi, N. González-Prelcic, and R. W. Heath, "IEEE 802.11ad-based radar: An approach to joint vehicular communicationradar system," *IEEE Trans. Veh. Technol.*, vol. 67, no. 4, pp. 3012–3027, April 2018.
- [4] E. Grossi, M. Lops, L. Venturino, and A. Zappone, "Opportunistic radar in IEEE 802.11ad networks," *IEEE Trans. Signal Process.*, vol. 66, no. 9, pp. 2441–2454, May 2018.
- [5] P. Kumari, M. E. Eltayeb, and R. W. Heath, "Sparsity-aware adaptive beamforming design for IEEE 802.11ad-based joint communicationradar," in *Proc. IEEE Radar Conf.*, April 2018, pp. 0923–0928.
- [6] P. Kumari, K. U. Mazher, A. Mezghani, and R. W. Heath, "Low resolution sampling for joint millimeter-wave MIMO communicationradar," in *Proc. IEEE Statistical Signal Processing Workshop (SSP)*, June 2018, pp. 193–197.
- [7] N. J. Myers, A. Mezghani, and R. W. Heath, "FALP: Fast beam alignment in mmwave systems with low-resolution phase shifters," *IEEE Transactions on Communications*, pp. 1–1, 2019.
- [8] M. Rossi, A. M. Haimovich, and Y. C. Eldar, "Spatial compressive sensing for MIMO radar," *IEEE Transactions on Signal Processing*, vol. 62, no. 2, pp. 419–430, Jan 2014.
- [9] R. W. Gerchberg, "A practical algorithm for the determination of phase from image and diffraction plane pictures," *Optik*, vol. 35, pp. 237–246, 1972.
- [10] H. Rauhut, "Compressive sensing and structured random matrices," Theoretical foundations and numerical methods for sparse recovery, vol. 9, pp. 1–92, 2010.
- [11] K. Li, L. Gan, and C. Ling, "Convolutional compressed sensing using deterministic sequences," *IEEE Transactions on Signal Processing*, vol. 61, no. 3, pp. 740–752, 2012.
- [12] E. Grossi, M. Lops, and L. Venturino, "A new look at the radar detection problem," *IEEE Transactions on Signal Processing*, vol. 64, no. 22, pp. 5835–5847, Nov 2016.
- [13] I. Gresham, A. Jenkins, R. Egri, C. Eswarappa, N. Kinayman, N. Jain, R. Anderson, F. Kolak, R. Wohlert, S. P. Bawell, J. Bennett, and J. P. Lanteri, "Ultra-wideband radar sensors for short-range vehicular applications," *IEEE Transactions on Microwave Theory and Techniques*, vol. 52, no. 9, pp. 2105–2122, Sept 2004.